Agricultural Systems 215 (2024) 103849

Contents lists available at ScienceDirect

Agricultural Systems

journal homepage: www.elsevier.com/locate/agsy

# A comprehensive assessment of yield loss in rice due to surface ozone pollution in India during 2005–2020: A great concern for food security

K.S. Anagha [a], Jayanarayanan Kuttippurath [a,*], Mamta Sharma [b], Juan Cuesta [c]

[a] CORAL, Indian Institute of Technology Kharagpur, Kharagpur 721302, India
[b] International Crops Research Institute for the Semi-Arid-Tropics (ICRISAT), Hyderabad 502324, India
[c] Univ Paris Est Creteil and Université Paris Cité, CNRS, LISA, F–94010 Créteil, France

## HIGHLIGHTS

- We analyse the yield loss in rice due to surface ozone pollution in India during 2005–2020.
- Rice production loss increased from 7.39 Million tonnes (Mt) in 2005 to 11.46 Mt. in 2020.
- An economic loss of $2.92 billion due to ozone pollution is estimated for the year 2020.
- This study has global implications as similar ozone pollution exists in many countries.

## GRAPHICAL ABSTRACT

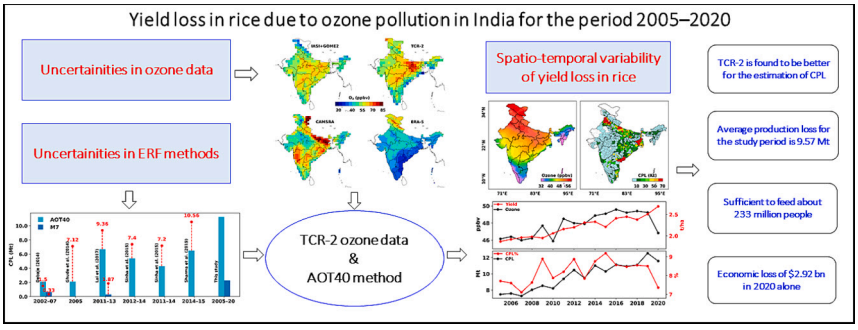


## ARTICLE INFO

Editor: Jagadish Timsina

*Keywords:*
Ozone pollution
Rice production
Yield loss
Economic loss
SDGs
Climate change
AOT40

## ABSTRACT

*CONTEXT:* About 60% of the world population relies primarily on rice as their staple food, and India ranks second in terms of global rice production. Studies have shown the adverse impact of surface ozone pollution on agriculture, particularly the yield loss (YL) of major staple crops.

*OBJECTIVE:* (i) To assess the bias associated with ozone data used for YL estimation, (ii) to find the uncertainties in ozone exposure/crop-response methods applied for computing YL and (iii) to analyse the spatio-temporal variability of YL in rice due to surface ozone in India for the period 2005–2020 to assess food security of the country.

*METHODS:* We use the Tropospheric Emission Spectrometer chemical reanalysis (TCR-2) surface ozone data and the ozone exposure/crop-response functions to compute YL in rice.

*RESULTS AND CONCLUSIONS:* By using the AOT40 crop-response method, we find a crop production loss (CPL) of about 7.39 million tonnes (Mt) of rice in 2005, which increased to 11.46 Mt. in 2020. The estimated average CPL for the study period is sufficient to feed about 233 million people per year. It also has incurred an economic loss of about $2.92 billion in 2020.

*SIGNIFICANCE:* Atmospheric pollution must be reduced to protect crop health and ensure food security, as evidenced by the two-fold rise of YL in rice due to ozone pollution during the past decade in India. This is also applicable to all agrarian economies of the world with high atmospheric pollution; reiterating the global significance of this study.

* Corresponding author at: CORAL, Indian Institute of Technology Kharagpur, 721302 Kharagpur, West Bengal, India.
*E-mail address:* jayan@coral.iitkgp.ac.in (J. Kuttippurath).

https://doi.org/10.1016/j.agsy.2023.103849
Received 15 March 2023; Received in revised form 24 December 2023; Accepted 25 December 2023
Available online 11 January 2024

## 1. Introduction

Air pollution is one of the important health and environmental concerns of current and future climate scenarios. Emissions of man-made pollutants have significantly increased since the beginning of industrial revolution (Houghton et al., 1995; Berntsen et al., 1997), and air quality in the developing countries has deteriorated over the period (Uglietti et al., 2015; World Health Organization, 2019; Shaddick et al., 2020; Kuttippurath et al., 2020; Fisher et al., 2021; Sicard et al., 2021). Reduction in air quality adversely affects climate, vegetation and ecosystem, and thus threatens public health and food security of the country. Several studies have shown that the exposure to high levels of pollutants such as $SO_2$, $NO_2$, $O_3$ and particulate matter (PM) can cause severe damage to crops (Agrawal et al., 2003; Balasubramanian et al., 2021). Furthermore, recent studies suggest that improved air quality could contribute to better agricultural yields and vegetation growth (Lobell and Burney, 2021; Kashyap et al., 2023).

Tropospheric ozone is the third most powerful greenhouse gas (GHG) after $CO_2$ and $CH_4$ (IPCC, 2021; Whaley et al., 2023) in terms of contribution to the total tropospheric radiative forcing (Dewan and Lakhani, 2022). It is a secondary air pollutant created by the photochemical reactions of its precursors, $CH_4$, $NO_x$, CO and Volatile organic compounds (VOCs). At the surface, ozone is considered as "bad ozone", because of its GHG effect and toxicity. Being a strong oxidant with the potential to generate photochemical smog, ozone disrupts human respiratory functioning and plant photosynthesis (West et al., 2006). Tropospheric ozone has been increasing in both hemispheres and even in Antarctica, attributed to the elevated anthropogenic emissions of its precursors and climate variability of the past few decades (e.g. Rathore et al., 2023; Kumar et al., 2021). As per various future projection studies, this state of rising concentrations of GHGs are expected to be continued world-wide, particularly in South and East Asia (Lelieveld and Dentener, 2000; Avnery et al., 2011; Chang et al., 2017). The annual mean surface ozone concentration in India has shown to be about 45.9 ppbv (ozone mixing ratio in parts per billion by volume), with its highest concentration in pre-monsoon (March–May: 54 ppbv) and lowest in summer (June–September: 40.5 ppbv) as observed by the Ozone Monitoring Instrument (OMI) and Tropospheric Emission Spectrometer (TES) (Lu et al., 2018). In the beginning of 21st century, ozone pollution has been identified as a severe health hazard (Zhang et al., 2019) and a major threat to food security, particularly in the developing Asian economies, including India (Burney and Ramanathan, 2014; Ghude et al., 2014).

As reported by the National Crop Loss Assessment Network (NCLAN) of the United Nations Environmental Protection Agency (US EPA), which is the first comprehensive and systematic investigation of the effects of $O_3$ on crops worldwide, tropospheric ozone has been recognised as the major atmospheric pollutant causing crop yield and biomass reduction (Lesser et al., 1990; Mauzerall and Wang, 2001; Feng et al., 2022). Surface ozone exposure at an increased rate and duration causes foliar injury to plants, impairing photosynthesis and lowering the productivity and yield of crops (Mauzerall and Wang, 2001; Ghude et al., 2014). After entering through the stomata of leaves, $O_3$ either reacts with the plasma membrane or transforms into numerous reactive oxygen species (ROS). This ROS can alter cellular activity, and eventually trigger cell death and premature senescence of leaves (Long and Naidu, 2002; Ainsworth, 2017). In addition, prior findings indicate that the nutritional quality, particularly carbohydrate, protein, calcium, magnesium and potassium, is declining in plants due to high ozone exposure (Singh and Agrawal, 2017). Henceforth, the yield of major crops such as rice, wheat and maize has also been reduced (Mills et al., 2007).

Loss of crop yield due to surface ozone is usually quantified with metrics based on the mean daytime ozone concentration (average of 7 h and 12 h daytime surface ozone concentration respectively for M7 and M12) and cumulative exposure (seasonally accumulated daytime ozone concentration above a threshold, i.e. AOT40, SUM06 and W126) (Tong et al., 2009). Among them, M7 and AOT40 are widely used for the studies in USA (Adams et al., 1985, 1989; Lesser et al., 1990; Wang and Mauzerall, 2004) and Europe (Mills et al., 2007), respectively. Van Dingenen et al. (2009) assessed the ozone induced crop damage for rice, maize, wheat and soybean globally by calculating AOT40 and M7 with the use of surface ozone simulated by an atmospheric chemical transport model (CTM), the Tracer Model version5 (TM5). They reported that rice and wheat are the most affected crops in terms of the estimated loss in production. The global economic loss for the crops under consideration in their study is between $14 and $26 billion (bn), with India and China together account for 40% of the loss. Tai et al. (2021) estimated that the current day globally aggregated yield loss for rice is 2.6 ± 0.8%. Feng et al. (2022) showed that hybrid rice would experience a higher relative yield loss (RYL) than that of inbred rice.

Carter et al. (2017) used field measurements to investigate the impact of increasing surface ozone on rice yield in the southeast China. They showed that, compared to a day with a maximum ozone concentration of <60 ppbv, an extra day with a peak ozone concentration of >120 ppbv is accountable for 1.1 ± 0.83% of yield loss in rice. The open-top chamber (OTC) study by Zhang et al. (2022) reported that yield loss (YL) of rice is higher, when the crop is exposed to ozone continuously during its entire growth period than that episodically during its different growth stages. A decrease in surface ozone causes increase in rice production by 9.8% in the absence of anthropogenic emissions, as observed in a sector-by-sector examination of air pollution impacts on rice in China (Xu et al., 2022). Out of the four sector-specific emission scenarios (industrial, energy, domestic and transportation), industrial emission management has been shown as the most effective and led to a 4.4% increase in rice production.

In a field-based study, Debaje (2014) calculated 3–16% YL of rabi rice in India from 2002 to 2007. Wheat was the most affected crop, followed by rice, according to a district-level calculation of the effect of ozone on major crops in India for the year 2005 by using the Weather Research and Forecasting with Chemistry (WRF-Chem version 3.2.2) CTM ozone simulations (Ghude et al., 2014). Their estimates are lower than that computed using the ozone simulated by global CTMs (Van Dingenen et al., 2009; Avnery et al., 2011). Ozone induced reduction in yield and quality also vary among the crop species (Tomer et al., 2015; Yadav et al., 2020; Yadav et al., 2021). Lal et al. (2017) estimated the RYL of 0.3–6.3% for rice, based on the surface ozone observations from 17 stations in India for the period of 2012–2013. They suggest the need for region-specific metrics and response relationships to estimate RYL in India and Southeast Asian countries. Sharma et al. (2019) estimated the nation-wide RYL of rice due to surface ozone as 6% by using the WRF-Chem model simulations of hourly ozone mixing ratios for the period 2014–2015. Their study highlights the necessity of long-term $O_3$ monitoring near croplands and establishment of a database for the annual emissions to facilitate policy decisions.

Indo Gangetic Plain (IGP), commonly known as the "breadbasket of India", is facing the problem of decline in crop productivity due to the increasing surface $O_3$ concentrations (Singh et al., 2018), which is a major concern for food security of the country. It is challenging to feed the nation's huge population sustainably and meet United Nation's Sustainable Development Goal 2 (UN SDG2) by 2030 in the context of rising pollution, population growth and changes in regional climate. However, the connection between air pollution and crop YL is less discussed in the Indian context, as most studies deal with urban air pollution and public health. Furthermore, previous studies considered very similar growing period for rice in all Indian states for the computation of YL (e.g. Ghude et al., 2014; Lal et al., 2017; Sharma et al., 2019). Nevertheless, there are regional differences in the rice-growing seasons and that should be considered in the calculations. The uncertainties associated with the available long-term fine resolution surface ozone reanalysis and satellite data are also need to be addressed. Therefore, objectives of this study are (i) a detailed error analysis of the ozone data used for the YL calculation, (ii) find the uncertainties associated with different ozone exposure/crop-response functions applied for the YL

computation and (iii) make a comprehensive analysis of YL in rice caused by ozone pollution for the period 2005–2020 and asses the associated food security of India.

## 2. Data

### 2.1. Ozone and crop production data

We have used different ozone datasets for the computation of YL and have examined the uncertainties associated with them to find the suitable data for the long-term crop production loss (CPL) assessment (detailed error analysis is presented in Section 4.1 and Supplementary Section S1). These data include Copernicus Atmosphere Monitoring Service Reanalysis (CAMSRA) (Inness et al., 2019), fifth generation European Center for Medium range Weather Forecast (ECMWF) reanalysis ERA-5 (Hersbach et al., 2020), the updated Tropospheric Chemistry Reanalysis and emission estimates version 2 (TCR-2), and the Infrared Atmospheric Sounding Interferometer plus Global Ozone Monitoring Experiment2 (IASI+GOME2) measurements (Cuesta et al., 2013).

The ERA-5 hourly ozone mixing ratio data are available from 1940 to date on 37 pressure levels from surface to 1 hPa at a horizontal resolution of 0.25° x 0.25°. Different ozone satellite data are assimilated in the ERA-5 reanalysis model to create the ozone profiles (Hersbach et al., 2020) with an updated version of Cariolle and Deque ozone parameterisation (Cariolle and Teyssedre, 2007). The CAMSRA 3-hourly ozone, produced using 4DVar data assimilation of the Integrated Forecasting System (IFS) by ECMWF, is available from 2003 to 2022 at a spatial resolution of 0.75° x 0.75° on 25 vertical levels from surface to 1 hPa. Here, the 3-hourly CAMSRA ozone data at 1000 hPa is interpolated to the hourly interval to calculate CPL.

The synergetic satellite multispectral approach for ozone, called IASI+GOME2, is developed at the Laboratoire Inter-universitaire des Systèmes Atmosphériques (LISA) laboratory, France. The IASI thermal infrared (TIR) and GOME-2 ultraviolet (UV) measurements combined together to get the tropospheric ozone below the altitude of 3 km (Cuesta et al., 2013). The Centre National d'Etudes Spatiales (CNES), France, in collaboration with the European Organisation for the Exploitation of Meteorological Satellites (EUMETSAT), developed the IASI instrument for operational meteorology and atmospheric chemistry monitoring (Boynard et al., 2018). It performs measurements on a horizontal resolution of 12 km across a swath width of about 2200 km, and these data are available since its launch in 2006. One of the new generation European sensors on the Meteorological Operational (MetOp) satellite series, GOME-2, was developed by the European Space Agency to measure UV radiation, trace gases and ozone. GOME-2 provides daily global coverage with a spatial resolution (80 km × 40 km) coarser than IASI, but a swath width comparable to IASI (for MetOp-A at around 09:30 AM local time) (Boynard et al., 2018). The GOME-2 ozone data are available from its launch date on 19 October 2006. The combined IASI+GOME2 provides a single vertical profile of the lowermost tropospheric ozone partial columns integrated between the surface and 3 km of altitude. It is obtained for every pixel at the IASI horizontal resolution by fitting co-located IR and UV spectra together, and this multi spectral retrievals show enhanced sensitivity to near surface ozone as compared to other single band approaches (Cuesta et al., 2013). For instance, there is a good qualitative agreement between the near-surface ozone pollution outbreak across East Asia as shown by in situ measurements and IASI+GOME2 retrievals, but it is not captured by the IASI-only retrievals (Cuesta et al., 2018). These data are validated with global ozonesondes and surface in situ ozone measurements in East Asia (Cuesta et al., 2018) and Europe (Cuesta et al., 2022; Okamoto et al., 2023), and are suitable for lower tropospheric ozone studies.

The TCR-2 reanalysis is available for the period 2005–2021 at 1.1° resolution. This reanalysis was created by incorporating several satellite ozone measurements [TES version 6 and Microwave Limb Sounder (MLS) version 4.2] (Bowman et al., 2006). Its processing was carried out using the global coupled CTM, MIROC-CHASER (Model of Interdisciplinary Research On Climate-Chemical Atmospheric general circulation model for Study of atmospheric Environment and Radiative forcing), to simulate emissions, wet and dry depositions, and tracer transport with comprehensive photochemistry in the troposphere and stratosphere (Miyazaki et al., 2020). To accurately describe ozone chemistry in the troposphere, it considers the basic chemical cycles of $O_x$-$NO_x$-$HO_x$-$CH_4$-CO and oxidation of Non-Methane Volatile Organic Compounds (NMVOCs). Measurements from a number of independent surface and aircraft sources have been used to validate the accuracy of this reanalysis (e.g. Miyazaki et al., 2020). Furthermore, 9 out of the 32 vertical levels of TCR-2 are within the lower troposphere, below 3 km altitude (Okamoto et al., 2023). As hourly surface ozone is necessary to calculate the ozone exposure metrics, we interpolated the 2-hourly TCR-2 data to the required intervals. To compute the district-wise production loss, these data are spatially interpolated to 0.25° resolution.

District-wise rice production and yield data for the study period (2005–2020) from the Special Data Dissemination Standard-Directorate of Economics and Statistics (SDDS-DES, Ministry of Agriculture Government of India) are used to estimate CPL.

## 3. Methods

### 3.1. Study region and crop seasons

We carry out a long-term (2005–2020) analysis of surface ozone exposure-related YL in rice, and associated national-level economic loss in India. According to the Directorate of Rice Development (Ministry of Agriculture and Farmer's Welfare), rice is cultivated during three seasons in India: autumn, winter and summer. The crop harvest season determines the name of these seasons, but sowing date varies slightly from one state to the other depending on local weather. The major rice-growing season in India, referred to as kharif or winter rice, begins in June or July and ends with harvesting in November or December. Around 84% of the rice production in India is during this season. Rabi rice (summer rice) is sown between November and February, and harvested between March and June. Pre-kharif (autumn) rice is sown from May to August, and harvested in September or October, but it is limited to some of the southern (e.g. Kerala and Tamilnadu), eastern (Orissa and West Bengal) and northeastern states in India. Details of seasons, sowing and harvesting months considered in our analysis based on the information given in Rice knowledge management portal (http://www.riceportal.in/research-domain/rice-state-wise) are provided in Supplementary Table TS1. The National Food Security Mission (NFSM) categorized rice-growing areas into five major divisions, namely the Southern (SR), Northern (NR), Western (WE), Eastern (EA) and Northeastern (NE) regions (see Fig. S1).

### 3.2. Ozone exposure metrics

The 7 h (09:00–16:00 h) mean surface $O_3$ concentration (M7) and accumulated daytime (08:00–20:00 h) hourly ozone concentration >40 ppbv (AOT40) for the entire crop-growing season are the main exposure metrics used for YL computations (Van Dingenen et al., 2009; Sinha et al., 2015; Lal et al., 2017). The AOT40 metric is the weighted sum that signifies higher ozone values to represent the pollution, but M7 gives equal weight to all ozone values, below 40 ppbv too (Sinha et al., 2015). Studies show that any agricultural crop should expect a 5% reduction in yield if the total combined surface ozone concentration in the growing period exceeds 3000 ppb.h (parts per billion. hour) (Mauzerall and Wang, 2001; Ishii et al., 2007). The Eqs. (1) and (2) for calculating exposure metrics are taken from Van Dingenen et al. (2009);

$$M7 = \frac{1}{n}\sum_{i=0}^{n} Ci \quad (1)$$

$$AOT40 = \sum_{i=0}^{n} (Ci - 40) \quad (2)$$

Here, 'n' is the total number of daylight hours in the entire crop growing season (09:00–16.00 h for M7 and 08.00–20.00 h for AOT40), and $C_i$ is daytime hourly ozone concentration for M7 and daytime hourly ozone concentration $\geq$ 40 ppbv for AOT40.

#### 3.2.1. Exposure-response functions

The exposure-response functions (ERF) are equations that quantify response of the crop, when exposed to specific levels of ozone and its impact on the crop yield (Mauzerall and Wang, 2001). In the early European and American OTC studies, ERF for each metric was calculated by fitting linear or Weibull functions (in turn for AOT40 and M7) to the yield responses of crops at different ozone concentrations. The absolute yield at zero ozone exposure was calculated first for each of these functions using regression analysis of the yield relative to ozone exposure (Mills et al., 2007). The relative yield (RY) for each exposure metric was then determined as the difference from the absolute yield, for which a value less than one indicates decrease in the yield (Avnery et al., 2011; Sinha et al., 2015). Here, we use the ERF relationship developed from the European and American OTC studies (Eqs. 3 and 4) to compute RY of rice. At each grid, we estimate AOT40 and M7 for the state-wise growing seasons of rice in India (period starting from 15 days after sowing to 15 days before harvesting is considered) and calculate RY;

$$RY = (-0.0000039 \times AOT40) + 0.94 \text{ (Mills et al., 2007)} \quad (3)$$

$$RY = \frac{exp^{[-(M7/202)]^{2.47}}}{exp^{[-(25/202)]^{2.47}}} \text{ (Adams et al., 1989)} \quad (4)$$

Furthermore, we have used the newly developed ERF for Indian rice (Eqs. 5 and 6) by Sinha et al. (2015) for Punjab and Haryana states;

$$RY = (-0.00001 \times AOT40) + 0.95 \quad (5)$$

$$RY = \frac{exp^{[-(M7/86)]^{2.5}}}{exp^{[-(25/86)]^{2.5}}} \quad (6)$$

#### 3.2.2. Estimation of seasonal and annual crop production loss

RY at zero exposure is equal to 1 by scaling the ERF based on exposure metrics. RYL is the difference between actual yield (RY) and hypothetical yield (assumed to be 1) of the crop (Avnery et al., 2011), and then RYL and CPL are calculated as;

$$RYL_{season} = 1 - RY_{season} \quad (7)$$

$$CPL_{season} = \frac{RYL_{season}}{(1 - RYL_{season})} \times CP_{season} \quad (8)$$

Here, $RYL_{season}$ is the district-wise and seasonal average of RYL. $CP_{season}$ is the total district-wise seasonal crop production of the respective year.

We estimate RYL for some states separately because of the regional differences in growing and harvesting periods as per the available information. The remaining regions or states with similar crop-growing periods are taken together for calculating RYL. The CPL for each season and district India is computed by Eq. (3) and then nation-wide total annual CPL is calculated by adding CPL across all districts and seasons (Eq. 9). See Fig. S2; outline of steps involved in the computation of CPL.

$$CPL_{year} = CPL_{kharif} + CPL_{rabi} + CPL_{pre-kharif} \quad (9)$$

Percentage loss (CPL %) per year is estimated with the Eq. (10);

$$CPL\%_{year} = \left(\frac{CPL_{year}}{CP_{year} + CPL_{year}}\right) \times 100 \quad (10)$$

Finally, the economic cost loss (ECL) of CPL is estimated by multiplying CPL with the minimum support price (MSP), which has been set by the Indian government for each year. MSP is a form of support by the Government of India to the farmers to insure a minimum price for their produce during the periods of its down fall (Commission for Agricultural costs and prices https://cacp.dacnet.nic.in). The MSP data for paddy are available from 2010 onwards, and henceforth, the calculation of ECL is performed for the 2010–2020 period.

## 4. Results and discussion

### 4.1. Uncertainties in the ozone data

We have performed a detailed error analysis of ozone data used for the CPL calculation in this study and is presented in Section S1 in Supplementary data and Table TS2. For instance, Fig. 1 shows the season-wise distribution of surface ozone in India for the period of 2017–2021. As compared to the satellite data (IASI+GOME2), the TCR-2 and CAMSRA ozone distributions are comparable across the India land regions, but ERA-5 fails to reproduce the satellite measured features. Among the datasets, more reliable results with respect to the satellite observations are produced by TCR-2. CAMSRA shows higher ozone in the Third Pole (TP) and hilly region for most seasons. In addition, the west coast of India and head Bay of Bengal regions show anomalous values in December–February (winter) as compared to the satellite measurements. ERA-5 also shows anomalous ozone values, particularly in the northern India and TP. Also, we have made another comparison of surface ozone from these datasets for a randomly chosen day of 25 April 2018 (see Fig. S3) to further evaluate their reliability. Here, the TCR-2 reanalysis better compare with the observation of IASI+GOME2, and show matching patterns in the central, IGP and southern regions. Though CAMSRA shows similar pattern of IASI+GOME2 as observed in IGP and eastern regions, it has relatively higher values of ozone (> 70 ppbv).

Because of the limited description of tropospheric chemistry in ERA-5, its ozone data mostly represent the downward contribution of stratospheric ozone, which may explain the differences of ERA-5 with CAMSRA and TCR-2. The lower tropospheric ozone transport is difficult to capture by ERA-5, as it does not have a chemical transport model (Park et al., 2020), and thus, ERA-5 ozone based CPL calculations are generally smaller due to its lower ozone concentration in major agricultural regions. On the other hand, the agreement of IASI+GOME2 with TCR-2 is better than that of CAMSRA and ERA-5. However, IASI+GOME2 do not have hourly surface ozone data to compute CPL and are available only from July 2016. Therefore, we have not considered the CAMSRA, ERA-5 and IASI+GOME2 ozone for the CPL calculations. To test the robustness of TCR-2 ozone for CPL estimation, we also compared those data with ozonesonde measurements from Thiruvananthapuram (SR), Pune (WE) and New Delhi (NR) (see Fig. S4), for which the stations represent different regions of India. A detailed discussion on the comparison is presented in Supplementary data (Section S1). The comparisons yield good agreement between TCR-2 and ozonesonde at different stations. Based on these uncertainty analyses, we have selected the TCR-2 ozone data for the computation of CPL in this study,

### 4.2. Uncertainties associated with methods

There are different ER functions to compute CPL and most methods are region specific. Therefore, we made an assessment to select an appropriate method for the Indian region. To perform the analysis, we compiled all available studies in the past and compared to our estimates for the same region and year, although there are some differences such as the season length. Fig. 2 shows the comparison of mean CPL estimated by different studies and methods. Except Debaje (2014), which is for rabi rice, all other studies are for kharif rice, and our estimates are the sum of CPL in all three rice producing seasons in a year. Ghude et al. (2014), Sinha et al. (2015) and Sharma et al. (2019) have computed CPL

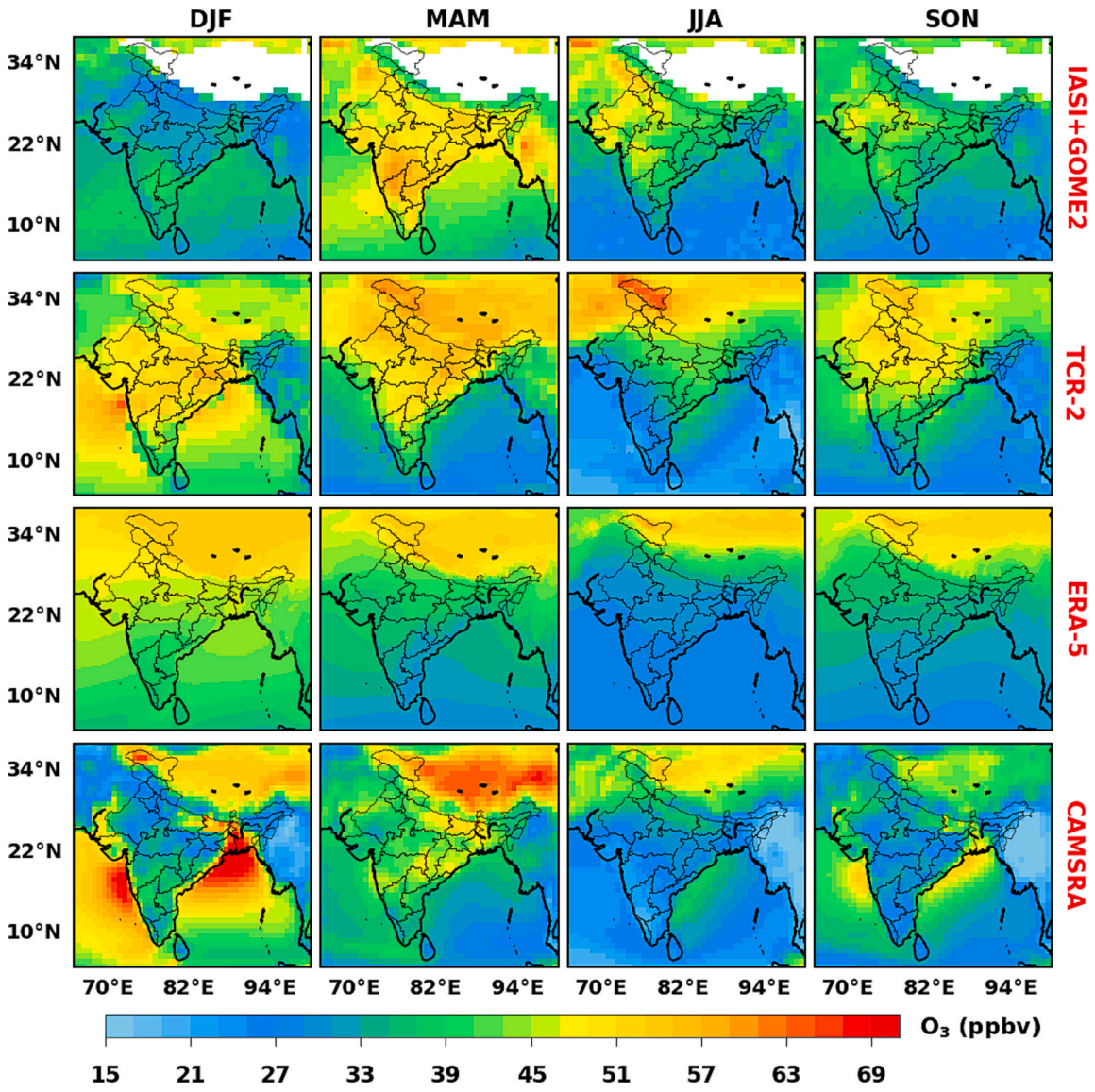


**Fig. 1.** Comparison of seasonal climatology of surface ozone mixing ratio (ppbv) from TCR-2, ERA-5 and CAMSRA ozone data with the IASI+GOME2 lower tropospheric ozone column integrated between the surface and 3 km altitude for the period 2017–2021. The TCR-2 data are available as surface ozone mixing ratios. The ERA-5 and CAMSRA available as ozone mixing ratio at pressure levels and we consider the 1000 hPa ozone. Each season is marked at the top panel of the respective column as DJF (December–February), MAM (March–May), JJA (June–August) and SON (September–November).

only with the AOT40 method, in which Sinha et al. (2015) used the ERF developed for the Punjab and Haryana regions together. All the other studies estimated CPL for the entire country. The red dots in the figure represent our estimates for the same period, season and method, as done in other studies. The mean CPL of rabi rice for the period 2002–2007 calculated by Debaje (2014) is 2.1 Mt. and 0.64 Mt., respectively, for AOT40 and M7. Our study period starts from 2005, and thus, the mean CPL for rabi rice for the period 2005–2007 is 1.5 Mt. by AOT40 and 0.33 Mt. by M7. Debaje (2014) used the AOT40 values derived from a linear relationship between AOT40 and M7 provided by Mills et al. (2007). However, the relationship between AOT40 and M7 is not linear, but exponential as described by Sinha et al. (2015). For this reason, the estimate by Debaje (2014) is higher than our estimates. In addition, the method of deriving AOT40 with such a linear relation may not be suitable for the Indian region (Sinha et al., 2015; Lal et al., 2017).

The other estimates show comparatively smaller CPL than our values (e.g. 0.3–6.7 Mt. for Lal et al., 2017, 2.1 Mt. for Ghude et al., 2014). The key reasons for the differences are: (i) the ozone data used in these studies are different, as the field studies use point measurements, but we use the best available satellite ozone. Since the computation is based on ozone data, the accuracy and resolution of ozone data are very important. In addition, the field studies mostly have ozone measurements in the urban and semi-urban sites, and thus, they cannot not fully capture the atmospheric chemistry in rural areas with croplands (e.g. Debaje, 2014; Lal et al., 2017; Sinha et al., 2015). Lower estimates of CPL could also result from ozone measurements distant from rural agricultural areas, which are likely to have higher concentrations (Sharma et al., 2019). (ii) The regional CTM based studies underestimate the observation based CPL, because of the difference in accuracy of the regional and local emission inventories used in the simulation of ozone in such models (Sharma et al., 2019). (iii) The differences in rice growing seasons, e.g. we have considered all seasons and there are changes in rice growing period among the states. (iv) Previous studies converted the district-wise crop yield data into grids of ozone resolution and then calculated RYL (e.g. Ghude et al., 2014; Sharma et al., 2019). However, the ozone and crop data resolution may be very coarse and then the interpolation could make uncertainties in the CPL calculation.

Among these studies, Sinha et al. (2015) used the information from

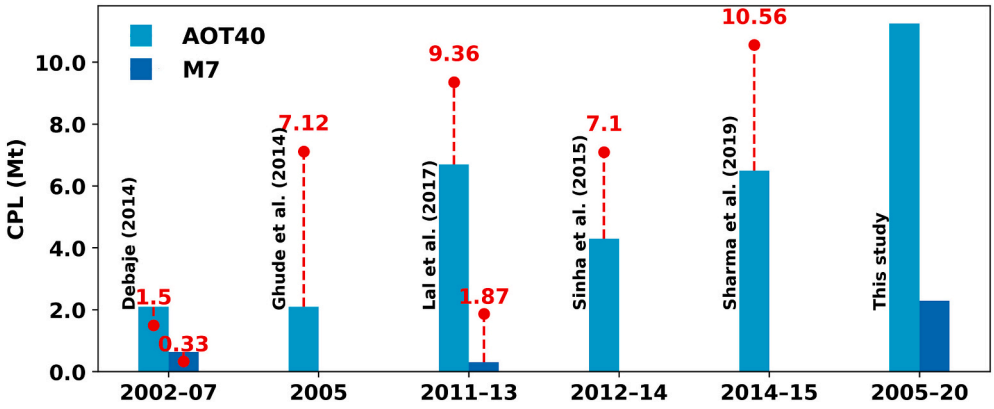


**Fig. 2.** Comparison of crop production loss (CPL in million tonnes) for rice estimated by different studies using the concentration based (AOT40 and M7) exposure response functions (ERF). Red dots representing the CPL obtained in our study for the same period of the corresponding study and red dash lines are the difference between the estimates. Debaje (2014) is for rabi rice (from December–February to March–June) and all other studies are for kharif rice (from June–July to November–December). Our study considers all seasons (including pre-kharif; from May–August to September– October). Sinha et al. (2015) used a new ERF to calculate CPL for Punjab and Haryana together. (For interpretation of the references to colour in this figure legend, the reader is referred to the web version of this article.)

peer-reviewed literature available for OTC studies on South Asian cultivars and verified their new ERF with ozone monitoring data from Mohali and the seeding experiment data conducted in Punjab and Haryana. Though the seeding experiments fortuitously exposed to different ozone levels as their sowing dates were different, the purpose of the experiments was not to study the impact of ozone on cultivars. Henceforth, the ozone monitoring and clean-air control treatments were absent in their experiment, and they used in situ ozone measurements at a suburban site in Mohali of Punjab (Sinha et al., 2015). The slope of their revised equation is steeper and intercept is lower than those reported by European OTC studies. This made the underestimation of CPL for the South Asian cultivars by the European (~10%) and American studies (~20%). The higher CPL by the new ERF derived by Sinha et al. (2015) can be attributed to the variant of cultivars, the comparatively higher sensitivity of Indian cultivars to ozone, and also the other reasons discussed above. Note that this ERF is also not applicable for the entire India.

In addition to the comparison of CPL by different ERF in previous studies, we have also performed a comparison of CPL calculated by different ozone data and ERF discussed in this study. Fig. 3 shows the CPL of kharif rice calculated with the European and American ERFs (Eqs. 3 and 4) and using the ERA-5, CAMSRA and TCR-2 data for the period 2017–2020. CPL calculated with AOT40 is smaller for ERA-5 (3.7–4.6 Mt) and CAMSRA (6.8–8.7 Mt) than that of TCR-2 (8.1–8.5 Mt) except for the year 2020, in which CPL by CAMSRA (8.7 Mt) is slightly higher than that of TCR-2 (8.5 Mt). By applying the M7 method, ERA-5 shows 0.2–0.3 Mt. and CAMSRA shows 0.85–1.17 Mt. CPL, which are lower than that of TCR-2 (1.67–1.89 Mt). Similar analysis with the ERF provided by Sinha et al. (2015) (Eqs. 5 and 6) is also performed (see Fig. S5), and the estimated CPL (e.g. about 15 Mt. for TCR-2, 12 Mt. for CAMSRA and 3.5 Mt. for ERA-5) is higher than that by Adams et al. (1989) and Mills et al. (2007) for both methods and all data sets, as discussed previously (Fig. 3). However, Sinha et al. (2015) show similar CPL values for both AOT40 and M7 with respect to the TCR-2 data. The ERF derived by Sinha et al. (2015) is most suitable for the north India, particularly Punjab and Haryana, and thus, it overestimates CPL for other regions. Furthermore, the comparison with previous studies, those use European and American ERF, shows that AOT40 provides better CPL estimates.

As already mentioned, since AOT40 is the weighted sum of daytime ozone concentration above a threshold, the loss estimated by this method will be higher than that based on the daytime averaged ozone between 09 h and 16 h (M7). The difference between CPL calculated with AOT40 and M7 is clearly visible in Fig. 2, Fig. 3, Fig. S5 and Fig. S6.

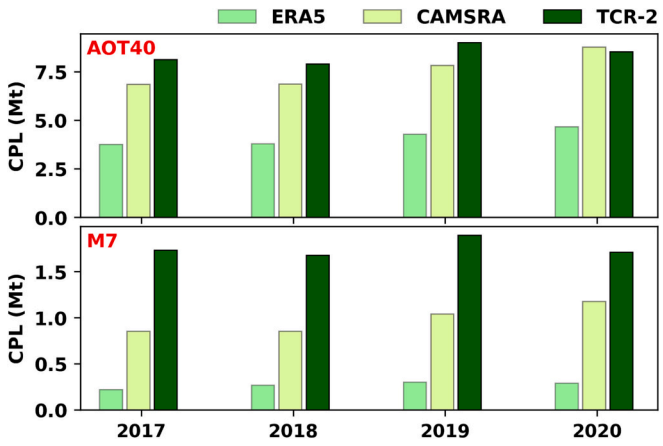


**Fig. 3.** Comparison of crop production loss (CPL) of kharif rice in million tonnes (Mt) calculated with exposure-response functions (ERF) provided by Mills et al. (2007) and Adams et al. (1989), respectively, for the AOT40 and M7 methods, and using the TCR-2, ERA-5 and CAMSRA surface ozone data for the period 2017–2020.

Additionally, AOT40 considers the impact of duration of ozone exposure on crops, whereas M7 solely depends on ozone concentration, and the AOT40 was developed to determine the grave detrimental effects of sporadic ozone pollution (Mills et al., 2007). Henceforth, AOT40 more accurately represents the substantial impact of ozone pollution on crops than M7 (Bui and Nguyen, 2023), and thus AOT40 has been used widely for estimating CPL (e.g. Ghude et al., 2014; Sinha et al., 2015; Sharma et al., 2019; Li et al., 2022). Therefore, based on these uncertainty assessments, we use the TCR-2 ozone data (as detailed in the previous section) and AOT40 method for the long-term assessment of CPL and associated economic loss in India.

### 4.3. Rice production and surface ozone concentration

Fig. 4 shows the district-wise spatial distribution of 16-year (2005–2020) average annual rice production in kilo tonnes (Kt) and annual climatology of daytime surface ozone. The major rice producing regions in India are IGP (Haryana, Punjab, Uttar Pradesh, Bihar and West Bengal) and eastern coastal states (Orissa, Andhra Pradesh and Tamilnadu), and they show a maximum district-wise production of ~1.1

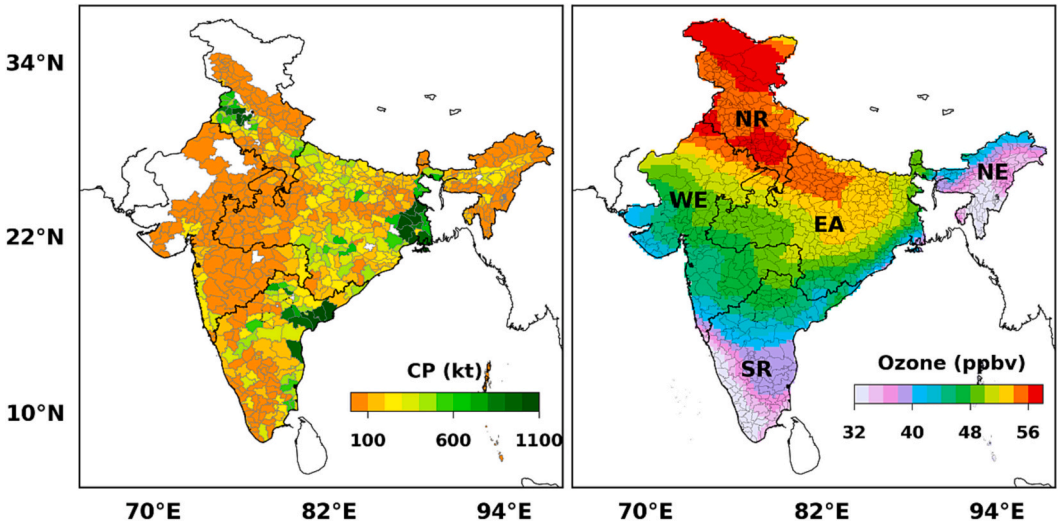


**Fig. 4.** District-wise annual rice production [CP – crop production in kilo tonnes (kt)] and daytime ozone mixing ratio (ppbv) in India averaged for the 2005–2020 period. Here, the regions are defined as, SR is Southern region, NR is Northern region, WE is Western region, EA is Eastern region and NE is Northeastern region.

Mt./yr. Almost all districts in Punjab produces 0.5–1 Mt. rice every year, where ozone is also higher, about 54–58 ppbv. Rest of the regions in IGP shows relatively higher ozone in the range of 48–54 ppbv. This higher ozone in IGP might be due to the high atmospheric pollution, reduced precipitation and intense solar radiation during the monsoon period, and due to dry weather in winter.

Fig. 5 shows the monthly average daytime surface ozone for the study period. North India, particularly IGP, shows ozone >55 ppbv in April and May. Ozone starts decreasing (25–30 ppbv) from April onwards in the southwestern coastal states. This ozone minimum gradually spreads to the central and southern regions (falling below 30 ppbv) from July to September (monsoon rain period). However, the monthly maximum of daytime ozone (Fig. S7) shows that there are days with values higher than 40 ppbv in all regions, even in summer monsoon. In the southwestern coastal region, only July–August show ozone lower than 40 ppbv, but not <30 ppbv. From September onwards, ozone again increases in the north India, which gradually extends to SR with comparatively lower values than that of NR. Post-monsoon season is the worst time of pollution with high ozone in IGP, mainly due to higher emissions of its precursors like biogenic NMVOCs, formaldehyde (HCHO) and $NO_x$, together with favorable meteorological conditions. Furthermore, IGP and some regions of the central and eastern states of India have very high ozone during March–May, which is mostly associated with elevated carbon monoxide (Kunchala et al., 2022). On the other hand, the southern tip of SR and some parts of NE experience less exposure to ozone compared to other regions. In fact, SR, particularly the southwestern region, is more humid and warmer than the northern region, which might have resulted in higher OH and increased photolysis of $NO_2$ (Rathore et al., 2023). Additionally, SR has relatively fewer point sources of pollution, such as lower vehicular emissions and biomass burning. Therefore, besides the unfavorable meteorological conditions, the lower amount of $NO_2$ also leads to reduced tropospheric ozone production in SR (Rathore et al., 2023).

Temporal evolution of the annual average rice yield and daytime surface ozone in different rice growing regions and seasons are depicted in Fig. S8 (kharif), Fig. S9 (rabi) and Fig. S10 (pre-kharif). The rabi and pre-kharif season yield in SR have increased consistently after 2015, at about 0.052 ± 0.004 (trend and the 95% confidence interval) tonnes/ha/year (t/ha/yr) and 0.090 ± 0.001 t/ha/yr, respectively. The corresponding ozone trend values are in turn 0.372 ± 0.055 ppbv/yr and 0.244 ± 0.051 ppbv/yr for pre-kharif and rabi seasons. NR also shows positive trend for these seasons, but smaller than that in SR. The decrease in yield is accompanied by an increase in ozone in most years. All regions and seasons show an increasing trend in yield and daytime ozone, except NE during pre-kharif, where a nonsignificant negative trend of ozone (−0.006 ± 0.053) is estimated. The EA (kharif and rabi seasons) and SR (rabi and pre-kharif) regions exhibit higher positive trends in yield and ozone. Our analysis shows that surface ozone is increasing in EA, at 0.214 ± 0.052 ppbv/yr. This finding is comparable to the annual trend of 0.218 ppbv/yr estimated for the eastern India for the period of 2003–2019 by Kunchala et al. (2022). Additionally, we find the highest positive trend in surface ozone in SR during all seasons, and are consistent with the findings of Rathore et al. (2023) for the tropospheric ozone.

During kharif season, North India, including IGP shows AOT40 values of 12,000–28,000 ppb.h, which makes the crops extremely susceptible to damage (Fig. 6). In contrast, the SR and EA exhibit AOT40 concentrations between 2000 and 4000 ppb.h during the kharif season. This could be associated with monsoon rains, cloud cover and other weather conditions discussed previously. Note that, the threshold of 40 ppbv is a cutoff, which signifies YL inflicted by episodes of very high surface ozone. It does not suggest that concentrations below 40 ppbv are not perilous for crop health. Prolonged exposure to ozone may negatively impact crops even at lower concentrations because it directly damages the cells that surround leaf stomata, and thus, reduce their ability to open and close (Hollaway et al., 2012). Additionally, the OTC studies reveal that the ozone levels below 40 nmol/mol impair paddy cultivars in South Asia (Sinha et al., 2015). Higher AOT40 values in kharif are primarily found in the western IGP and hilly regions. Approximately 15,000–22,000 ppb.h of AOT40 is observed in the remaining states of northern India and also in some parts of EA and WE. During rabi season, there observed a higher AOT40 (26000–34,000 ppb.h) area stretches from IGP to the eastern, central and western India. In this season, ozone is equally elevated in the northern areas of SR. The areas with higher AOT40 observed during rabi in the north and central India are confined only to IGP during pre-kharif season (22000–280,000 ppb.h). Mittal et al. (2007) also reported that AOT40 was higher than 3000 ppb.h in most regions of India during spring and summer months of 2000.

### 4.4. Rice production loss and economic loss

The spatial representation of the 16-year average district-wise annual CPL and temporal changes in all India total annual CPL of rice due to ozone for the study period (Fig. S6 top panel and bottom panel respectively) show that the AOT40 method provides a maximum

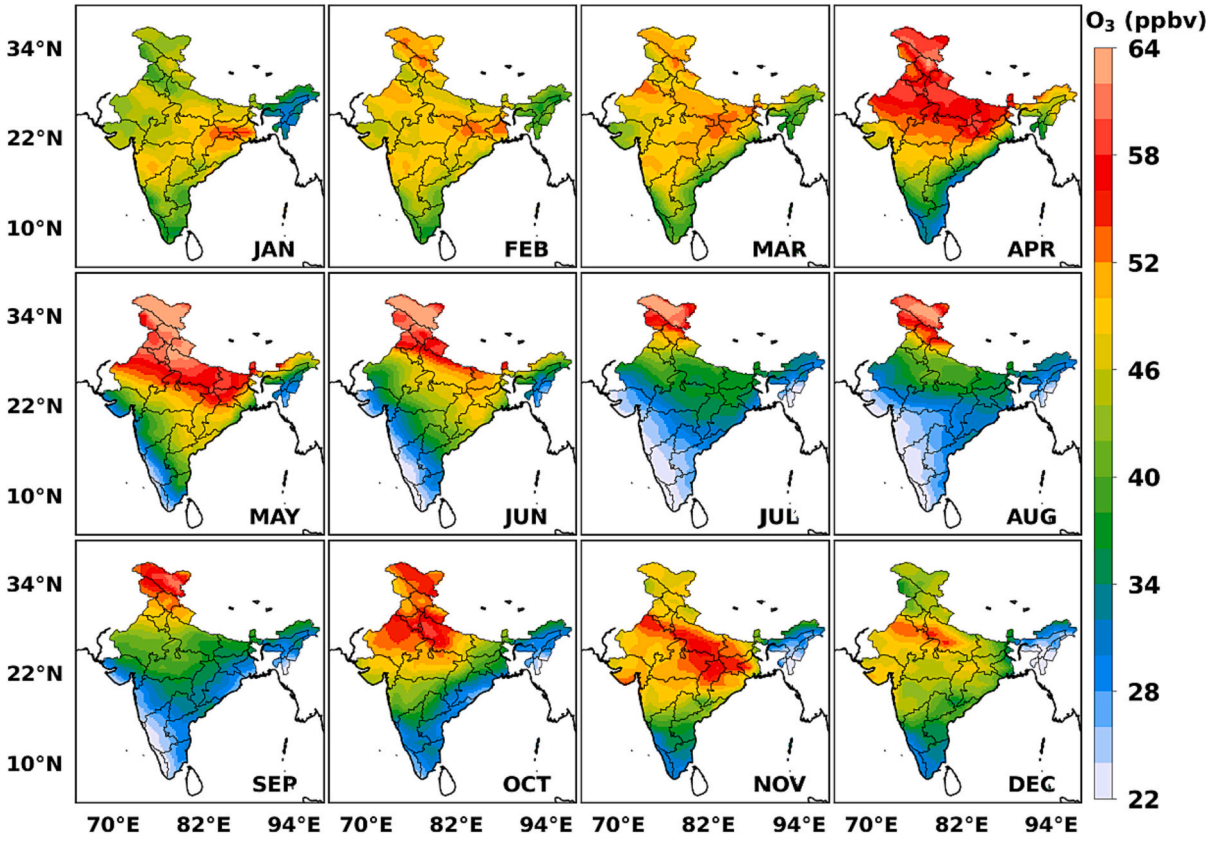


**Fig. 5.** Monthly climatology of the daytime (08.00–20.00 h) average surface ozone mixing ratio (ppbv) using the TCR-2 data for the 2005–2020 period. The months are represented by their first three letters (e.g. JAN is January and DEC is December).

district-wise CPL of around 0.9 Mt. EA and NR (including IGP) show higher production loss, in which Punjab, West Bengal, Uttar Pradesh (UP), Bihar, Chhattisgarh, Andhra Pradesh and eastern parts of Madhya Pradesh have contributed more to the total CPL. The total annual CPL of the study period is 7.18–12.42 Mt., which generally shows an increasing trend, except for a few years (e.g. reduced loss in 2007, 2010, 2013 and 2020). Those years may have been affected by the changes in either the amount of ozone or the harvesting area and production.

The time series of yearly average of surface ozone, yield of rice, CPL and percentage loss of rice due to ozone (CPL%) are shown in Fig. 7. All India yearly average daytime surface ozone (Fig. 7 top) increases from 46 to 50 ppbv for the study period, although there is a small decrease of ozone in the years 2007, 2010, 2013 and 2020. The average yield also shows an increase from 2005 to 2020, except in the drought years of 2009 and 2014–2015. According to Mishra et al. (2020), concurrent hot and dry monsoon of recent decades occurred in the years 2009, 2014 and 2015. Furthermore, 2009 was a flash drought year and that was widespread in India, particularly in the central, northeastern and Himalaya regions. In addition, ozone concentration was also higher in those years. Note that the yield of rice during the COVID-19 lockdown period (2019–2020) has further increased, and these might have contributed by the overall reduction in surface ozone. Since tropospheric ozone is a secondary air pollutant, its formation depends on the precursor concentrations, which are region specific (e.g. Gopikrishnan et al., 2022). Therefore, the increase or decrease cannot be generalised with all India ozone average. The annual average yield of rice varies

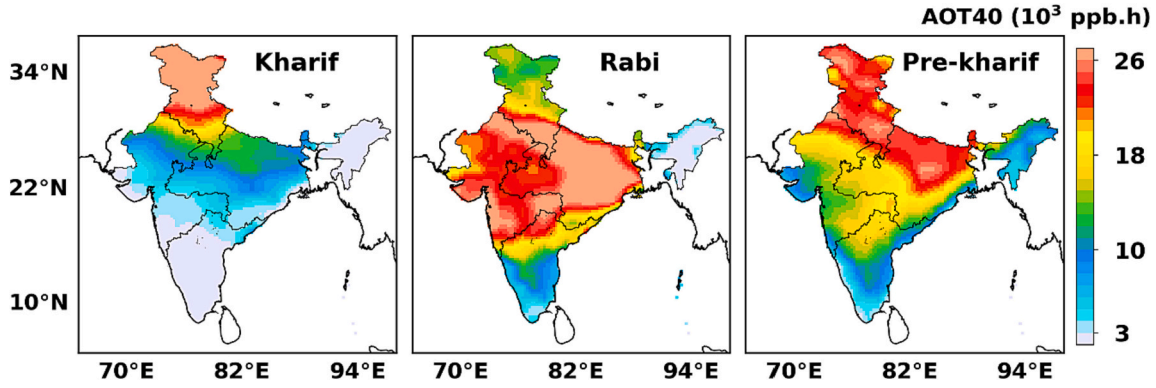


**Fig. 6.** Climatology of AOT40 (ppb.h) during the kharif (from sowing in June–July to harvesting in November–December), rabi (from December–February to March–June) and pre-kharif (from May–August to September– October) seasons using the TCR-2 surface ozone data in India for the 2005–2020 period. Different rice producing regions in India are also marked.

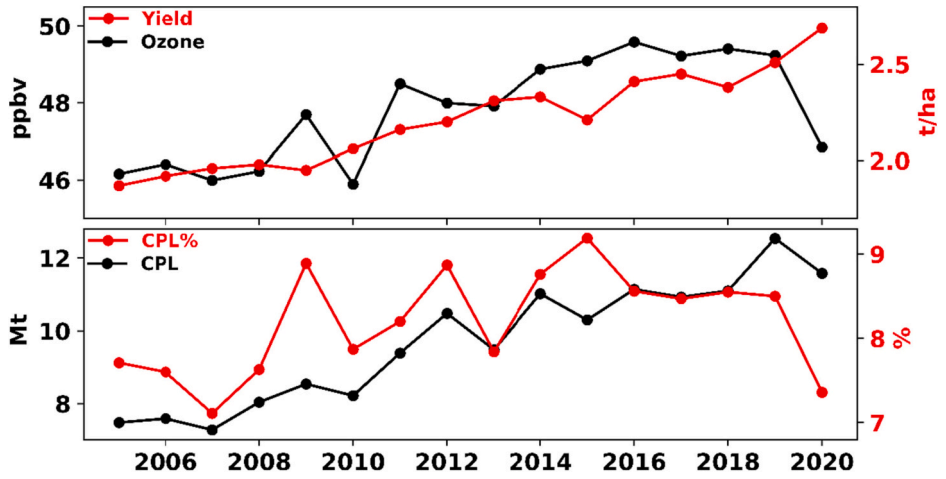


**Fig. 7.** Top. Temporal evolution of annual average daytime surface ozone (ppbv) and annual average yield of rice in tonnes/ha (t/ha). Bottom. Annual crop production loss (CPL in million tonnes) and percentage loss (CPL%) of rice due to ozone exposure estimated using the AOT40 method for the period 2005–2020. Here, the rice yield and production data are taken from the Special Data Dissemination Standard-Directorate of Economics and Statistics (SDDS-DES, Ministry of Agriculture Government of India), and ozone data from the TCR-2 chemical reanalysis. The CPL and CPL% are calculated based on the AOT40 method.

from 1.5 to 2.6 t/ha. It has increased rapidly since 2009 as a result of advanced technology in agriculture (Kuttippurath and Kashyap, 2023), but production loss has also increased because of the rise in ozone pollution near the croplands. The CPL and CPL% of rice (Fig. 7 bottom) for each year estimated by AOT40 method shows 7.18–12.42 Mt. and 7–9.5%, respectively, for the study period. The highest CPL% values are found in the years 2009 (9%), 2012 (8.8%) and 2015 (9.5%), which can be attributed to the higher ozone during the period.

Fig. 8 shows the total rice production loss due to surface ozone in the five rice cultivating regions of India (2005–2020) for the kharif, rabi and pre-kharif seasons. Corresponding AOT40 values are given in Fig. S11. The production loss of kharif rice is higher in EA followed by NR, whereas that of rabi and pre-kharif rice are higher in EA and SR. Lal et al. (2017) also observed that the highest annual loss in rice due to ozone is in the eastern region. In kharif, NR is exposed to higher amount of AOT40 (>15,000 ppb.h) followed by EA (>5000 ppb.h except for 2006 and 2007, Fig. S11). Rabi season AOT40 is higher in all regions, particularly in EA and NR, and pre-kharif and rabi AOT40 in SR and NE are also higher (8000–10,000 ppb.h) compared to that in kharif.

Economic damage increases each year simultaneously with the CPL, except for some years (e.g. 2007, 2010, 2013 and 2020) that show slightly lower values of CPL than that of previous year due to small decline in ozone. Our analysis shows that the ozone-induced crop damage in India made an economic loss of $2.92 bn in 2020 alone. Our study estimates a nationwide total loss in rice production averaged for the study period as 9.57 Mt., which could have used to feed about 233 million people in all those years.

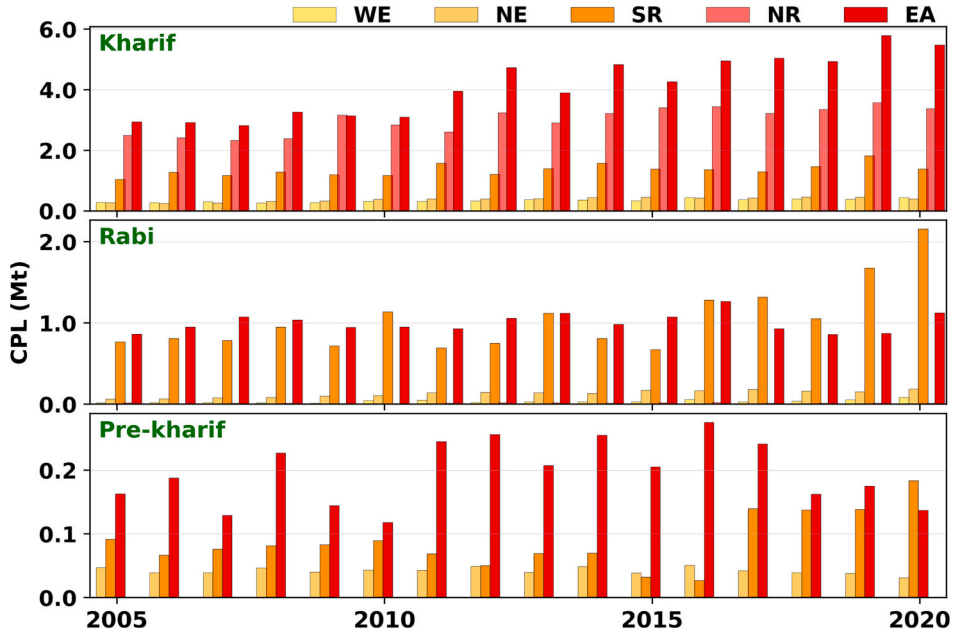


**Fig. 8.** Region-wise production loss due to surface ozone estimated using the TCR-2 ozone data and AOT40 method for the kharif (from sowing in June–July to harvesting in November–December), rabi (from December–February to March–June) and pre-kharif (from May–August to September– October) rice in India from 2005 to 2020. Here, the regions are defined as, SR is Southern region, NR is Northern region, WE is Western region, EA is Eastern region and NE is Northeastern region.

## 5. Limitations and future scope

The yield response of rice to surface ozone concentration in this study is computed iusing the crop-specific ERF derived from the early OTC studies in North America and Europe. In those studies, the ambient or filtered air, that is nearly identical to field measurements, is treated with elevated ozone concentrations (Adams et al., 1985; Mills et al., 2007). Here, the effects of all other variables on rice yield are expressed as the yield at zero ozone dose, and it still lacks a thorough analysis of the notable differences between the environmental conditions of OTC, where the experiments were conducted, and the actual natural conditions in the surroundings. It neglects the influence of local weather and phenotypical and genotypical factors on regulating the response of crop to ozone. Therefore, these can contribute some uncertainty in the RYL estimation. According to recent studies, the RYL of rice obtained from ozone exposure experiments in Asia is higher than that derived from experiments carried out in North America and Europe. Additionally, the high-yielding hybrid rice varieties exhibit much higher RYL compared to the inbred varieties (e.g. Feng et al., 2022). In fact, different cultivars have varied response to ozone as reported by the Asian OTC studies (e.g. Sawada and Kohno, 2009; Yadav et al., 2020; Yadav et al., 2021). This could also introduce some uncertainty in the CPL estimates as ERF does not consider different rice breeds. Furthermore, the impact of ozone on plants depends on the stomatal conductance of leaves that control ozone absorption, besides the influence of ambient ozone concentration. Recent developments in the flux-based metric, Phytotoxic ozone dose over an hourly flux threshold of Y nmol/$m^2$/s (PODy) consider the influence of biological and environmental factors on plant stomatal ozone absorption. The Deposition of Ozone for Stomatal Exchange ($DO_3SE$) model provides stomatal conductance algorithm and flux-based parameterisations for computing YL in wheat and potato, and therefore, further research is needed in this direction for rice and other cultivars. It is also important to consider the ozone exposure during various growth stages of the cultivar, including particular attention to the actual vegetative growth stages and the periods of seed germination and maturation.

The accuracy of surface ozone measurements, particularly in the proximity to the crop canopy height, is necessary for assessing its sensitivity to plants. It depends on a number of factors, including its precursor emissions, variability in ozone between urban and rural locations, and the ratio of $NO_x$ to VOC. However, the number of ground-based instruments located in agricultural fields are insufficient for the estimation of RYL now. Although satellite measurements cover rural areas and have global coverage, most of these do not have hourly frequency for the computation of exposure metrics. Among the ozone datasets, TCR-2 performs better, but more surface measurements with a wide network are necessary for accurate estimates of RYL. In addition, the agricultural land use map rather than the administrative boundaries might provide better estimates of the regional changes in CPL.

## 6. Conclusions

We conduct a long-term analysis of the reduction in Indian rice yield caused by surface ozone exposure. Based on the availability of ozone measurements, response functions and rice production data, loss in rice production at district level over the past 16 years (2005–2020) is calculated. Yield loss due to ozone depends on the ozone data, method, regions and seasons considered for the estimation. Among the ERA-5, CAMSRA and TCR-2 surface ozone datasets, the TCR-2 is found to be better for the estimation of CPL as revealed by the comparisons, including the IASI+GOME2 satellite multispectral data and ozonesonde measurements. Similarly, a thorough analysis of different ERFs is also performed and AOT40 method is found to be better suited for the CPL calculations. Using the TCR-2 surface ozone data and AOT40 method, the highest district-level production loss of ~0.9 Mt. per year is found in the major rice producing areas of IGP (Punjab, Haryana, UP, Bihar and West Bengal) and eastern coastal states (Orissa, Andhra Pradesh and Tamilnadu). In Punjab, most districts produce between 0.5 and 1.1 Mt. of rice annually. However, the crop is extremely susceptible to damage due to the higher daytime surface ozone of about 46–54 ppbv there. The remaining regions in IGP have daytime surface ozone of 44–58 ppbv during different seasons, but highest in summer (56–58 ppbv). The CPL induced by ozone pollution causes an ECL between $1.77 and $3.15 bn per annum, as estimated for recent decade (2010−2020). This ECL is solely attributable to the CPL due to ozone, but there are several other costs associated with the entire cultivation process; starting with the actual preparation of the land to the harvest. The estimated ECL can be even higher, when the total cost for the entire processes is considered. In this context, it is necessary to mitigate air pollution for sustainable crop production and food security in India, and ozone pollution need to be regularly monitored to prepare for agriculture production and its management.

## Funding

This study received no funding.

## CRediT authorship contribution statement

**K.S. Anagha:** Writing – original draft, Visualization, Validation, Software, Methodology, Investigation, Formal analysis, Data curation. **Jayanarayanan Kuttippurath:** Writing – review & editing, Writing – original draft, Visualization, Supervision, Resources, Project administration, Methodology, Investigation, Funding acquisition, Formal analysis, Conceptualization. **Mamta Sharma:** Writing – review & editing, Investigation, Formal analysis, Data curation. **Juan Cuesta:** Writing – review & editing, Investigation, Formal analysis, Data curation.

## Declaration of Competing Interest

The authors declare no conflict or competing interest.

## Data availability

TCR-2 Chemical reanalysis surface ozone mixing ratio data is available at the website of NASA Jet Propulsion Laboratory (JPL) Chemical Reanalysis Products. https://doi.org/10.25966/9qgv-fe81.

District-wise seasonal rice production data is available at the Ministry of Agriculture and Farmers welfare SDDS–DES website, https://data.desagri.gov.in/website/crops-apy-report-web.

IASI+GOME2 data use in this study is available at https://iasi.aeris-data.fr/o3_iago2/

Rice knowledge management portal. http://www.riceportal.in/research-domain/rice-state-wise (accessed 11 October 2022).

National Food Security Mission (NFSM) https://www.nfsm.gov.in/ (accessed 11 October 2022).

United Nations Sustainable Development Goals. https://www.un.org/sustainabledevelopment/ hunger/ (accessed 12 September 2022).

Directorate of rice development. https://drdpat.bih.nic.in/ (accessed 10 August 2022).

Commission for Agricultural costs and prices (CACP) https://cacp.dacnet.nic.in (accessed 15 September 2022).

CAMSRA data: https://www.ecmwf.int/en/research/climate-reanalysis/cams-reanalysis

ERA–5 data: https://www.ecmwf.int/en/forecasts/datasets/reanalysis-datasets/era5

## Acknowledgements

We thank the Director, Indian Institute of Technology Kharagpur (IIT KGP), Chairman of CORAL IIT KGP and the Science and Engineering Research Board (SERB) for facilitating the study (The Core Research

Grant). We thank the JPL for providing surface ozone data and the Ministry of Agriculture for providing district-wise seasonal crop production data. The authors acknowledge the AERIS data infrastructure for providing access to the IASI+GOME2 data in this study and LISA for the development of the retrieval algorithms.

## Appendix A. Supplementary data

Supplementary data to this article can be found online at https://doi.org/10.1016/j.agsy.2023.103849.

## References


Adams, R.M., Hamilton, S.A., McCarl, B.A., 1985. An assessment of the economic effects of ozone on US agriculture. JAPCA 35 (9), 938–943. https://doi.org/10.1080/00022470.1985.10465981.

Adams, R.M., Glyer, J.D., Johnson, S.L., McCarl, B.A., 1989. A reassessment of the economic effects of ozone on US agriculture. JAPCA 39 (7), 960–968. https://doi.org/10.1080/08940630.1989.10466583.

Agrawal, M., Singh, B., Rajput, M., Marshall, F., Bell, J.N.B., 2003. Effect of air pollution on peri-urban agriculture: a case study. Environ. Pollut. 126 (3), 323–329. https://doi.org/10.1016/S02697491(03)00245-8.

Ainsworth, E.A., 2017. Understanding and improving global crop response to ozone pollution. Plant J 90 (5), 886–897. https://doi.org/10.1111/tpj.13298.

Avnery, S., Mauzerall, D.L., Liu, J., Horowitz, L.W., 2011. Global crop yield reductions due to surface ozone exposure: 2. Year 2030 potential crop production losses and economic damage under two scenarios of $O_3$ pollution. Atmos. Environ. 45 (13), 2297–2309. https://doi.org/10.1016/j.atmosenv.2011.01.002.

Balasubramanian, S., Domingo, N.G., Hunt, N.D., Gittlin, M., Colgan, K.K., Marshall, J. D., Robinson, A.L., Azevedo, I.M., Thakrar, S.K., Clark, M.A., Tessum, C.W., 2021. The food we eat, the air we breathe: a review of the fine particulate matter-induced air quality health impacts of the global food system. Environ. Res. Lett. 16 (10), 103004. https://doi.org/10.1016/j.atmosenv.2011.01.002.

Berntsen, T.K., Isaksen, I.S., Myhre, G., Fuglestvedt, J.S., Stordal, F., Larsen, T.A., Freckleton, R.S., Shine, K.P., 1997. Effects of anthropogenic emissions on tropospheric ozone and its radiative forcing. J. Geophys. Res. Atmos. 102 (D23), 28101–28126. https://doi.org/10.1029/97JD02226.

Bowman, K.W., Rodgers, C.D., Kulawik, S.S., Worden, J., Sarkissian, E., Osterman, G., Steck, T., Lou, M., Eldering, A., Shephard, M., Worden, H., 2006. Tropospheric emission spectrometer: retrieval method and error analysis. IEEE Trans. Geosci. Remote Sens. 44 (5), 1297–1307. https://doi.org/10.1109/TGRS.2006.871234.

Boynard, A., Hurtmans, D., Garane, K., Goutail, F., Hadji-Lazaro, J., Koukouli, M.E., Wespes, C., Vigouroux, C., Keppens, A., Pommereau, J.P., Pazmino, A., 2018. Validation of the IASI FORLI/EUMETSAT ozone products using satellite (GOME-2), ground-based (Brewer–Dobson, SAOZ, FTIR) and ozonesonde measurements. Atmos. Meas. Tech. 11 (9), 5125–5152. https://doi.org/10.5194/amt-11-5125-2018.

Bui, L.T., Nguyen, P.H., 2023. Assessment of rice yield and economic losses caused by ground-level $O_3$ exposure in the Mekong delta region, Vietnam. Heliyon 9 (7), e17883. https://doi.org/10.1016/j.heliyon.2023.e17883.

Burney, J., Ramanathan, V., 2014. Recent climate and air pollution impacts on Indian agriculture. Proc. Natl. Acad. Sci. U. S. A. 111 (46), 16319–16324. https://doi.org/10.1073/pnas.1317275111.

Cariolle, D., Teyssedre, H., 2007. A revised linear ozone photochemistry parameterization for use in transport and general circulation models: multi-annual simulations. Atmos. Chem. Phys. 7 (9), 2183–2196. https://doi.org/10.5194/acp-7-2183-2007.

Carter, C.A., Cui, X., Ding, A., Ghanem, D., Jiang, F., Yi, F., Zhong, F., 2017. Stage-specific, nonlinear surface ozone damage to rice production in China. Sci. Rep. 7, 44224. https://doi.org/10.1038/srep44224.

Chang, K.L., Petropavlovskikh, I., Cooper, O.R., Schultz, M.G., Wang, T., 2017. Regional trend analysis of surface ozone observations from monitoring networks in eastern North America, Europe and East Asia. Elem. Sci. Anth. 5 https://doi.org/10.1525/elementa.243.

Cuesta, J., Eremenko, M., Liu, X., Dufour, G., Cai, Z., Höpfner, M., von Clarmann, T., Sellitto, P., Forêt, G., Gaubert, B., Beekmann, M., 2013. Satellite observation of lowermost tropospheric ozone by multispectral synergism of IASI thermal infrared and GOME-2 ultraviolet measurements over Europe. Atmos. Chem. Phys. 13 (19), 9675–9693. https://doi.org/10.5194/acp-13-9675-2013.

Cuesta, J., Kanaya, Y., Takigawa, M., Dufour, G., Eremenko, M., Foret, G., Miyazaki, K., Beekmann, M., 2018. Transboundary ozone pollution across East Asia: daily evolution and photochemical production analysed by IASI+ GOME2 multispectral satellite observations and models. Atmos. Chem. Phys. 18 (13), 9499–9525. https://doi.org/10.5194/acp-18-9499-2018.

Cuesta, J., Costantino, L., Beekmann, M., Siour, G., Menut, L., Bessagnet, B., Landi, T.C., Dufour, G., Eremenko, M., 2022. Ozone pollution during the COVID-19 lockdown in the spring of 2020 over Europe analysed from satellite observations, in situ measurements, and models. Atmos. Chem. Phys. 22 (7), 4471–4489. https://doi.org/10.5194/acp-22-4471-2022.

Debaje, S.B., 2014. Estimated crop yield losses due to surface ozone exposure and economic damage in India. Environ. Sci. Pollut. Res. 21, 7329–7338.

Dewan, S., Lakhani, A., 2022. Tropospheric ozone and its natural precursors impacted by climatic changes in emission and dynamics. Front. Environ. Sci. 10, 2499. https://doi.org/10.3389/fenvs.2022.1007942.

Feng, Z., Xu, Y., Kobayashi, K., Dai, L., Zhang, T., Agathokleous, E., Calatayud, V., Paoletti, E., Mukherjee, A., Agrawal, M., Park, R.J., 2022. Ozone pollution threatens the production of major staple crops in East Asia. Nat. Food 3 (1), 47–56. https://doi.org/10.1038/s43016-021-00422-6.

Fisher, S., Bellinger, D.C., Cropper, M.L., Kumar, P., Binagwaho, A., Koudenoukpo, J.B., Park, Y., Taghian, G., Landrigan, P.J., 2021. Air pollution and development in Africa: impacts on health, the economy, and human capital. Lancet Planet Health 5 (10), E681–E688. https://doi.org/10.1016/S2542-5196(21)00201-1.

Ghude, S.D., Jena, C., Chate, D.M., Beig, G., Pfister, G.G., Kumar, R., Ramanathan, V., 2014. Reductions in India's crop yield due to ozone. Geophys. Res. Lett. 41 (15), 5685–5691. https://doi.org/10.1002/2014GL060930.

Gopikrishnan, G.S., Kuttippurath, J., Raj, S., Singh, A., Abbhishek, K., 2022. Air quality during the COVID–19 lockdown and unlock periods in India analyzed using satellite and ground-based measurements. Environ. Process. 9, 28. https://doi.org/10.1007/s40710-022-00585-9.

Hersbach, H., Bell, B., Berrisford, P., Hirahara, S., Horányi, A., Muñoz-Sabater, J., Nicolas, J., Peubey, C., Radu, R., Schepers, D., Simmons, A., 2020. The ERA5 global reanalysis. Q. J. R. Meteorol. Soc. 146 (730), 1999–2049. https://doi.org/10.1002/qj.3803.

Hollaway, M.J., Arnold, S.R., Challinor, A.J., Emberson, L.D., 2012. Intercontinental trans-boundary contributions to ozone-induced crop yield losses in the Northern Hemisphere. Biogeosciences 9 (1), 271–292. https://doi.org/10.5194/bg-9-271-2012.

Houghton, J.T., Meira Filho, L.G., Bruce, J., Lee, H., Callander, B.A., Haites, E., Harris, N., Maskell, K. (Eds.), 1995. Climate Change 1994: Radiative Forcing of Climate Change and an Evaluation of the IPCC 1992 IS92 Emission Scenarios. Cambridge University Press.

Inness, A., Ades, M., Agustí-Panareda, A., Barré, J., Benedictow, A., Blechschmidt, A.M., Dominguez, J.J., Engelen, R., Eskes, H., Flemming, J., Huijnen, V., 2019. The CAMS reanalysis of atmospheric composition. Atmos. Chem. Phys. 19 (6), 3515–3556. https://doi.org/10.5194/acp-19-3515-2019.

IPCC, 2021. Climate Change. In: Masson-Delmotte, V., Zhai, P., Pirani, A., Connors, S.L., Péan, C., Berger, S., Caud, N., Chen, Y., Goldfarb, L., Gomis, M.I., Huang, M., Leitzell, K., Lonnoy, E., Matthews, J.B.R., Maycock, T.K., Waterfield, T., Yelekçi, O., Yu, R., Zhou, B. (Eds.), The Physical Science Basis, Contribution of Working Group I to the Sixth Assessment Report of the Intergovernmental Panel on Climate Change. Cambridge UniversityPress. Tech. rep. https://www.ipcc.ch/report/ar6/wg1/{#}FullReport.

Ishii, S., Bell, J.N.B., Marshall, F.M., 2007. Phytotoxic risk assessment of ambient air pollution on agricultural crops in Selangor State, Malaysia. Environ. Pollut. 150 (2), 267–279. https://doi.org/10.1016/j.envpol.2007.01.012.

Kashyap, R., Kuttippurath, J., Patel, V.K., 2023. Improved air quality leads to enhanced vegetation growth during the COVID–19 lockdown in India. Appl. Geogr. 151, 102869 https://doi.org/10.1016/j.apgeog.2022.102869.

Kumar, P., Kuttippurath, J., von Der Gathen, P., Petropavlovskikh, I., Johnson, B., McClure-Begley, A., Cristofanelli, P., Bonasoni, P., Barlasina, M.E., Sánchez, R., 2021. The increasing surface ozone and tropospheric ozone in Antarctica and their possible drivers. Environ. Sci. Technol. 55 (13), 8542–8553. https://doi.org/10.1021/acs.est.0c08491.

Kunchala, R.K., Singh, B.B., Karumuri, R.K., Attada, R., Seelanki, V., Kumar, K.N., 2022. Understanding the spatiotemporal variability and trends of surface ozone over India. Environ. Sci. Pollut. Res. 29 (4), 6219–6236. https://doi.org/10.1007/s11356-021-16011-w.

Kuttippurath, J., Kashyap, R., 2023. Greening of India: forests or croplands? Appl. Geogr. 161 https://doi.org/10.1016/j.apgeog.2023.103115.

Kuttippurath, J., Singh, A., Dash, S.P., Mallick, N., Clerbaux, C., Van Damme, M., Clarisse, L., Coheur, P.F., Raj, S., Abbhishek, K., Varikoden, H., 2020. Record high levels of atmospheric ammonia over India: spatial and temporal analyses. Sci. Total Environ. 740, 139986 https://doi.org/10.1016/j.scitotenv.2020.139986.

Lal, S., Venkataramani, S., Naja, M., Kuniyal, J.C., Mandal, T.K., Bhuyan, P.K., Kumari, K. M., Tripathi, S.N., Sarkar, U., Das, T., Swamy, Y.V., 2017. Loss of crop yields in India due to surface ozone: estimation based on a network of observations. Environ. Sci. Pollut. Res. 24, 20972–20981. https://doi.org/10.1007/s11356-017-9729-3.

Lelieveld, J., Dentener, F.J., 2000. What controls tropospheric ozone? J. Geophys. Res. Atmos. 105 (D3), 3531–3551. https://doi.org/10.1029/1999JD901011.

Lesser, V.M., Rawlings, J.O., Spruill, S.E., Somerville, M.C., 1990. Ozone effects on agricultural crops: statistical methodologies and estimated dose-response relationships. Crop Sci 30 (1), 148–155. https://doi.org/10.2135/cropsci1990.0011183X003000010033x.

Li, D., Shindell, D., Ding, D., Lu, X., Zhang, L., Zhang, Y., 2022. Surface ozone impacts on major crop production in China from 2010 to 2017. Atmos. Chem. Phys. 22 (4), 2625–2638. https://doi.org/10.5194/acp-22-2625-2022.

Lobell, D.B., Burney, J.A., 2021. Cleaner air has contributed one-fifth of US maize and soybean yield gains since 1999. Environ. Res. Lett. 16, 074049 https://doi.org/10.1088/1748-9326/ac0fa4.

Long, S.P., Naidu, S.L., 2002. Effects of oxidants at the biochemical, cell and physiological levels, with particular reference to ozone. Air Pollut. Plant Life 2, 69–88.

Lu, X., Zhang, L., Liu, X., Gao, M., Zhao, Y., Shao, J., 2018. Lower tropospheric ozone over India and its linkage to the south Asian monsoon. Atmos. Chem. Phys. 18 (5), 3101–3118. https://doi.org/10.5194/acp-18-3101-2018.

Mauzerall, D.L., Wang, X., 2001. Protecting agricultural crops from the effects of tropospheric ozone exposure: reconciling science and standard setting in the United States, Europe, and Asia. Annu. Rev. Environ. Resour. 26, 237–268.
Mills, G., Hayes, F., Jones, M.L.M., Cinderby, S., 2007. Identifying ozone-sensitive communities of (semi-) natural vegetation suitable for mapping exceedance of critical levels. Environ. Pollut. 146 (3), 736–743. https://doi.org/10.1016/j.envpol.2006.04.005.
Mishra, V., Thirumalai, K., Singh, D., Aadhar, S., 2020. Future exacerbation of hot and dry summer monsoon extremes in India. npj Clim. Atmos. Sci. 3, 1–9. https://doi.org/10.1038/s41612-020-0122-4.
Mittal, M.L., Hess, P.G., Jain, S.L., Arya, B.C., Sharma, C., 2007. Surface ozone in the Indian region. Atmos. Environ. 41 (31), 6572–6584. https://doi.org/10.1016/j.atmosenv.2007.04.035.
Miyazaki, K., Bowman, K.W., Yumimoto, K., Walker, T., Sudo, K., 2020. Evaluation of a multi-model, multi-constituent assimilation framework for tropospheric chemical reanalysis. Atmos. Chem. Phys. 20 (2), 931–967. https://doi.org/10.5194/acp-20-931-2020.
Okamoto, S., Cuesta, J., Beekmann, M., Dufour, G., Eremenko, M., Miyazaki, K., Boonne, C., Tanimoto, H., Akimoto, H., 2023. Impact of different sources of precursors on an ozone pollution outbreak over Europe analysed with IASI+ GOME2 multispectral satellite observations and model simulations. Atmos. Chem. Phys. 23 (13), 7399–7423. https://doi.org/10.5194/acp-23-7399-2023.
Park, S., Son, S.W., Jung, M.I., Park, J., Park, S.S., 2020. Evaluation of tropospheric ozone reanalyses with independent ozonesonde observations in East Asia. Geosci. Lett. 7, 1–12. https://doi.org/10.1186/s40562-020-00161-9.
Rathore, A., Gopikrishnan, G.S., Kuttippurath, J., 2023. Changes in tropospheric ozone over India: variability, long-term trends and climate forcing. Atmos. Environ. 309, 119959 https://doi.org/10.1016/j.atmosenv.2023.119959.
Sawada, H., Kohno, Y., 2009. Differential ozone sensitivity of rice cultivars as indicated by visible injury and grain yield. Plant Biol. 11 (s1), 70–75. https://doi.org/10.1111/j.1438-8677.2009.00233.x.
Shaddick, G., Thomas, M.L., Mudu, P., Ruggeri, G., Gumy, S., 2020. Half the world's population are exposed to increasing air pollution. npj Clim. Atmos. Sci. 3, 1–5. https://doi.org/10.1038/s41612-020-0124-2.
Sharma, A., Ojha, N., Pozzer, A., Beig, G., Gunthe, S.S., 2019. Revisiting the crop yield loss in India attributable to ozone. Atmos. Environ. X 1, 100008. https://doi.org/10.1016/j.aeaoa.2019.1000 08.
Sicard, P., Agathokleous, E., De Marco, A., Paoletti, E., Calatayud, V., 2021. Urban population exposure to air pollution in Europe over the last decades. Environ. Sci. Eur. 33, 1–12. https://doi.org/10.1186/s12302-020-00450-2.
Singh, A.A., Agrawal, S.B., 2017. Tropospheric ozone pollution in India: effects on crop yield and product quality. Environ. Sci. Pollut. Res. 24 (5), 4367–4382. https://doi.org/10.1007/s11356-016-8178-8.
Singh, A.A., Fatima, A., Mishra, A.K., Chaudhary, N., Mukherjee, A., Agrawal, M., Agrawal, S.B., 2018. Assessment of ozone toxicity among 14 Indian wheat cultivars under field conditions: growth and productivity. Environ. Monit. Assess. 190 (4), 1–14. https://doi.org/10.1007/s10661-018-6563-0.
Sinha, B., Singh Sangwan, K., Maurya, Y., Kumar, V., Sarkar, C., Chandra, B.P., Sinha, V., 2015. Assessment of crop yield losses in Punjab and Haryana using 2 years of continuous in situ ozone measurements. Atmos. Chem. Phys. 15 (16), 9555–9576. https://doi.org/10.5194/acp-15-9555-2015.
Tai, A.P., Sadiq, M., Pang, J.Y., Yung, D.H., Feng, Z., 2021. Impacts of surface ozone pollution on global crop yields: comparing different ozone exposure metrics and incorporating co-effects of $CO_2$. Front. Sustain. Food Syst. 5, 534616 https://doi.org/10.3389/fsufs.2021.534616.
Tomer, R., Bhatia, A., Kumar, V., Kumar, A., Singh, R., Singh, B., Singh, S.D., 2015. Impact of elevated ozone on growth, yield and nutritional quality of two wheat species in northern India. Aerosol Air Qual. Res. 15 (1), 329–340. https://doi.org/10.4209/aaqr.2013.12.0354.
Tong, D.Q., Mathur, R., Kang, D., Yu, S., Schere, K.L., Pouliot, G., 2009. Vegetation exposure to ozone over the continental United States: assessment of exposure indices by the eta-CMAQ air quality forecast model. Atmos. Environ. 43 (3), 724–733. https://doi.org/10.1016/j.atmosenv.2008.09.084.
Uglietti, C., Gabrielli, P., Cooke, C.A., Vallelonga, P., Thompson, L.G., 2015. Widespread pollution of the South American atmosphere predates the industrial revolution by 240 y. Proc. Natl. Acad. Sci. U. S. A. 112 (8), 2349–2354. https://doi.org/10.1073/pnas.1421119112.
Van Dingenen, R., Dentener, F.J., Raes, F., Krol, M.C., Emberson, L., Cofala, J., 2009. The global impact of ozone on agricultural crop yields under current and future air quality legislation. Atmos. Environ. 43 (3), 604–618. https://doi.org/10.1016/j.atmosenv.2008.10.033.
Wang, X., Mauzerall, D.L., 2004. Characterizing distributions of surface ozone and its impact on grain production in China, Japan and South Korea: 1990 and 2020. Atmos. Environ. 38 (26), 4383–4402.
West, J.J., Fiore, A.M., Horowitz, L.W., Mauzerall, D.L., 2006. Global health benefits of mitigating ozone pollution with methane emission controls. Proc. Natl. Acad. Sci. U. S. A. 103, 3988–3993. https://doi.org/10.1016/j.atmosenv.2004.03.067.
Whaley, C.H., Law, K.S., Hjorth, J.L., Skov, H., Arnold, S.R., Langner, J., Pernov, J.B., Bergeron, G., Bourgeois, I., Christensen, J.H., Chien, R.Y., 2023. Arctic tropospheric ozone: assessment of current knowledge and model performance. Atmos. Chem. Phys. 23 (1), 637–661. https://doi.org/10.5194/ac p-23-637-2023.
World Health Organization, 2019. World health statistics overview 2019: Monitoring health for the SDGs, sustainable development goals (No. WHO/DAD/2019.1) https://apps.who.int/iris/ bitstream/handle /10665 /31–1696/ WHO-DAD-2019.1-eng.pdf (accessed 20 August 2022).
Xu, J., Dong, X., Zhang, T., Liu, J., Tao, S., 2022. Mitigation of air pollutant impacts on rice yields in China by sector. Environ. Res. Lett. 17, 05403. https://doi.org/10.1088/1748-9326/ac681c.
Yadav, D.S., Mishra, A.K., Rai, R., Chaudhary, N., Mukherjee, A., Agrawal, S.B., Agrawal, M., 2020. Responses of an old and a modern Indian wheat cultivar to future $O_3$ level: physiological, yield and grain quality parameters. Environ. Pollut. 259, 113939 https://doi.org/10.1016/j.envpol.2020.11 3939.
Yadav, A., Bhatia, A., Yadav, S., Singh, A., Tomer, R., Harit, R., Kumar, V., Singh, B., 2021. Growth, yield and quality of maize under ozone and carbon dioxide interaction in North West India. Aerosol Air Qual. Res. 21 (2), 200194. https://doi.org/10.4209/aaqr.2020.05.0194.
Zhang, J., Wei, Y., Fang, Z., 2019. Ozone pollution: a major health hazard worldwide. Front. Immunol. 10, 2518. https://doi.org/10.3389/fimmu.2019.02518.
Zhang, G., Hu, Q., Cao, R., Fu, R., Risalat, H., Pan, X., Hu, Y., Shang, B., Wu, R., 2022. Yield loss in rice by acute ozone pollution could be recovered. Agric. Environ. Lett. 7 (2), e20093 https://doi.org/10.1002/ael2.20093.